Algorithm Theoretical Basis Document (ATBD)
Version 03-00

NASA Time-Resolved Observations of Precipitation structure and storm Intensity with a Constellation of Smallsats (TROPICS) Precipitation Retrieval and Profiling Scheme (PRPS)

Prepared for:
Time-Resolved Observations of Precipitation structure and storm Intensity with a Constellation of Smallsats (TROPICS) National Aeronautics and Space Administration (NASA)

Prepared by:

Chris Kidd and Toshi Matsui
UMD/ESSIC & NASA/GSFC
NASA/GSFC Code 612.0
Greenbelt, MD 20771

23 March 2022

TABLE OF CONTENTS

LIST OF FIGURES

LIST OF TABLES

1 INTRODUCTION

1.1 Objective

This document describes the precipitation algorithm and processing sequence for the Precipitation Retrieval and Profiling Scheme (PRPS) for the Time-Resolved Observations of Precipitation structure and storm Intensity with a Constellation of Smallsats (TROPICS) Millimeter-wave Soudner (TMS). This technique is intended to exploit the capabilities of this instrument and currently represents the initial post-launch version. As such, the technique described here, as the initial version of the scheme for this instrument, will have a number of known and unknown issues present in the product generated. Where possible these will be addressed and notes taken on improvements for implementation in future releases.

1.2 Revision History

Version	*Date*	*Author*	*Description*
00-00	30 April 2019	Chris Kidd & Toshi Matsui	Initial version of ATBD
00-01	19 November 2019	Chris Kidd & Toshi Matsui	Updated version to include pre-launch description of technique and results.
01-00	21 June 2021	Chris Kidd & Toshi Matsui	Final update on description of pre-launch retrieval scheme
02-00	07 March 2022	Chris Kidd & Toshi Matsui	Post-launch updates to document
03-00	23 March 2022	Chris Kidd & Toshi Matsui	ATBD update with latest results

2 OBSERVING SYSTEM

2.1 Role of Passive Microwave Sounding Instruments

The retrieval of precipitation from satellite-based sensors relies primarily upon visible, infrared, passive and active microwave instrumentation. While the active microwave instruments undoubtedly provide the most direct measure of satellite-based precipitation, such space-borne observations are currently confined to the GPM DPR and CloudSat CPR, and are thus are very much limited in time and space. Visible and infrared techniques are capable of providing estimates of precipitation at relatively fine temporal and spatial scale from geostationary (GEO) and low Earth orbiting (LEO) platforms, but such estimates are indirect since they rely on relationships between cloud-top characteristics and precipitation at the surface. Passive microwave (PMW) estimates fall between these two extremes with hydrometeors providing the main source of atmospheric attenuation and scattering. However, since PMW sensors only occupy LEOs, multiple sensors are required to provide sufficient temporal and spatial coverage.

While much work has been done on the extraction of precipitation information from passive microwave imaging (a.k.a. conical scanning) sensors, less work has been concentrated upon retrievals from sounding (a.k.a. cross-track) microwave instruments. However, work on the latter is critical for a) providing additional observations to meet the necessary sampling requirements for precipitation measurements, and b) for longer-term studies of future precipitation missions, particularly since the future of passive microwave radiometry currently rests largely upon sounding instruments on smaller satellite platforms.

This document refers specifically to the retrieval scheme for the passive microwave radiometer onboard the TROPICS suite of cubesats; pertinent information to this satellite and sensor is described below.

Table 1: Recent and present microwave sensors.

Satellite	Sensor	Channels	Retrieval resolution
Active microwave instruments			
GPM	DPR	13.6/35.5 GHz	5.4 x 5.4 km
TRMM	PR	13.6 GHz	4.3 x 4.3 km
Cloudsat	CPR	94 GHz	1.4 x 1.4 km
Passive microwave imagers			
GPM	GMI	10.7-183.31 GHz	10.9 x 18.1 km*
DMSP-F16 DMSP-F17 DMSP-F18 DMSP-F19	SSMIS	19.35-183.31 GHz	45 x 74 km*
GCOM-W1	AMSR2	6.7-89.0 GHz	14 x 22 km*
TRMM	TMI	10.7-89.0 GHz	20.9 x 34.6 km*
Passive microwave sounders			
NOAA-18 NOAA-19 METOPA METOPB	MHS	89.0-183.31 GHz	17.12 x 21.64 km*
NPP	ATMS	23.0-183.31 GHz	16.51 x 16.22 km*
MeghaTropiques	SAPHIR *SAPHIR*	183.31 GHz (x6)	7.34 x 7.27 km* *5.4 x 5.4 km#*
TROPICS	**TMS**	**91.7-204.8 GHz**	**15.2 x 15.2 km#**

* current GPROF retrieval resolutions (at nadir for sounders)
\# resolution of the PRPS retrieval scheme

2.2 The TROPICS mission

The Time-Resolved Observations of Precipitation structure and storm Intensity with a Constellation of Smallsats (TROPICS) mission will provide rapid-refresh microwave measurements over the Tropics that can be used to observe the thermodynamics of the troposphere and precipitation structure for storm systems at the mesoscale and synoptic scale over the entire storm lifecycle. TROPICS comprises an intial pathfinder cubesat mission in a Polar orbit (launched on 30 June 2021), to be followed by a constellation of cubesats in low inclination low-Earth orbits. Each cubesat will host a high-performance radiometer scanning across the satellite track at 30 RPM to provide temperature profiles using seven channels near the 118.75 GHz oxygen absorption line, water vapor profiles using 3 channels near the 183 GHz water vapor absorption line, imagery in a single channel at 91.665 GHz primarily for precipitation measurements, and a single channel at 204.8 GHz for cloud ice measurements.

This observing system offers an unprecedented temporal resolution to measure the atmospheric environment and inner-core conditions of tropical cyclones (TCs) over the entire Tropics and is a profound leap forward in the temporal resolution of several key parameters needed for detailed study of high-impact meteorological events. TROPICS will demonstrate that a constellation approach to Earth Science can provide improved resolution, configurable coverage (Tropics, near global, or global), flexibility, reliability, and launch access at extremely low cost, thereby serving as a model for future missions.

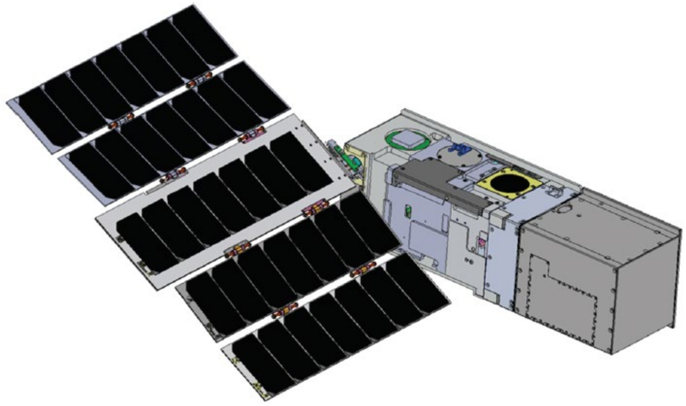

Figure 1: TROPICS cubesat showing the spacecraft bus, radiometer and deployed articulated solar array.

2.3 The TROPICS instrument

Comprehensive information about the TROPICS instrument can be found at Blackwell et al. (2018). This document provides a summary of the sensor relevant to the retrieval scheme.

The instrument provides observations across a 1779 km swath with a symmetrical scan pattern, i.e. equal number of field of views (FOVs) each side of nadir. Each scan line provides 81 scan positions; being a cross-track sensor these produce the finest resolution at nadir, becoming coarser towards the edge of scan. The instrument observes the Earth and atmosphere with channels primarily around the 118 GHz oxygen and 183.31 GHz water vapor bands, together with two channels at 91.655 and 204.8 GHz. Table 2 below shows the channel characteristics (together with the corresponding ATMS channels); note that for any scan position the spatial resolution varies with the observations frequency. Frequencies around 91.655 and 183.31 GHz have a good history of being utilized for precipitation retrievals, responding to the scattering of upwelling radiation by the ice particles within precipitating weather systems (Kidd et al. 2016). The addition of the 204.8 GHz extends this capability by improving the identification and classification of ice particles. While the 114-118 GHz (oxgen) channels relate primarily to temperature profiles of the atmosphere, these too can be potentially used for precipitation retrievals (Li et al 2018), and may allow the delineation of liquid/frozen precipitation.

Table 2: TMS and ATMS channel sets.

TMS Channel	Central frequency	Bandwidth	Effective resolution	NEΔT	ATMS Channel	Central frequency	Bandwidth	NEΔT
1	91.655±1.4 GHz	1000 MHz	50.7 km	0.95 K	16	89.5 GHz	5000 MHz	0.50 K
2	114.50 GHz	1000 MHz	41.2 km	0.55 K				
3	115.95 GHz	800 MHz	41.2 km	0.60 K				
4	116.65 GHz	600 MHz	41.2 km	0.70 K				
5	117.25 GHz	600 MHz	41.2 km	0.70 K				
6	117.80 GHz	500 MHz	41.2 km	0.75 K				
7	118.24 GHz	380 MHz	41.2 km	0.85 K				
8	118.58 GHz	300 MHz	41.2 km	1.00 K				
9	184.41 GHz	2000 MHz	27.5 km	0.60 K	22	183.31±1.0	500 MHz	0.90 K
10	186.51 GHz	2000 MHz	27.5 km	0.60 K	20	183.31±3.0	1000 MHz	0.80 K
11	190.31 GHz	2000 MHz	27.5 km	0.60 K	18	183.31±7.0	2000 MHz	0.80 K
12	204.8 GHz	2000 MHz	26.0 km	0.60 K				

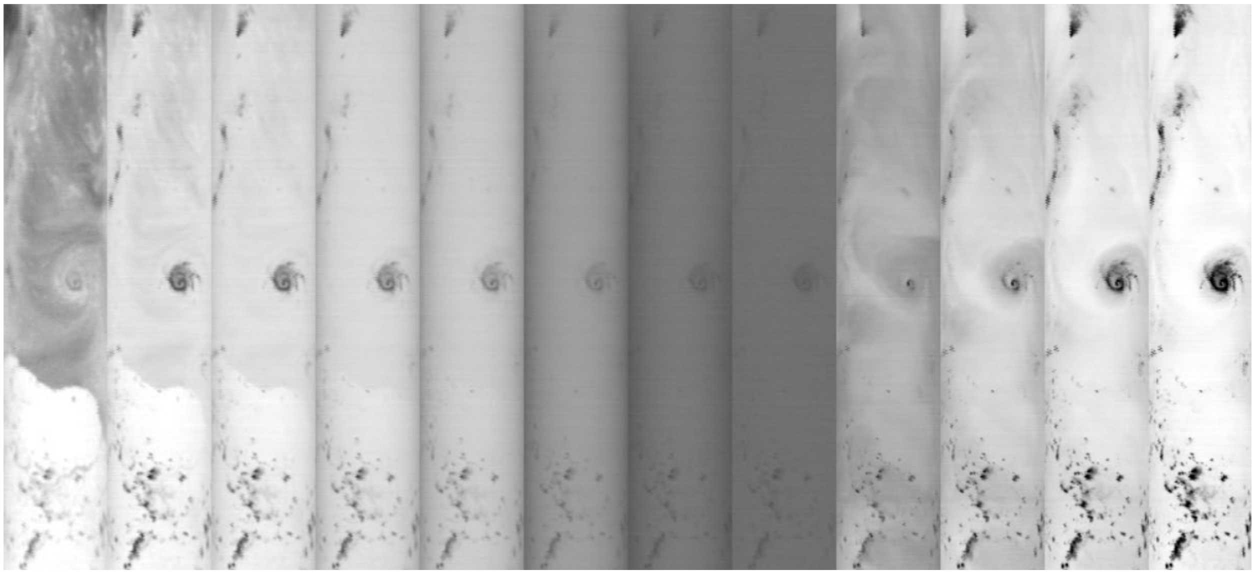

Figure 2: Example of the 12 channels of the TROPICS sensor ranging from 91.655 (left) through to 204.8 GHz (right) for Hurricane Sam on 27 September 2021. The time at the center of image is 17:49 UTC with a location of about 16°N 52°W. Data is extracted from TROPICS01.BRTT.L1B.Orbit01352.V02-03.ST20210927-170942.ET20210927-184458.CT20220208-174340.nc

2.4 Algorithm considerations

An important consideration for the retrieval of precipitation from the available channels is that the relationship between the observed Tbs and surface precipitation is not necessarily direct. This is due to the fact that these frequencies directly relate to ice particles, water vapor, and/or temperature profiles at the middle-to-upper levels of the atmosphere, rather than near the surface. In particular, the 183.31 GHz channels relate to emissions from water vapor in the cloud-less atmospheric column: decreases in the Tbs is usually indicative of greater concentrations of water vapor, causing the sensitivity to 'peak' higher in the atmosphere, hence lower temperatures. However, the 183.31 GHz channels are also sensitive to the scattering of upwelling microwave radiation by ice particles in cloud and/or by precipitation systems, the latter of which is exploited here to identify precipitation. The 114-118 GHz (O_2) channels respond to atmospheric temperature profiles since these channels are sensitive to oxygen: these channels offer the prospect of not only being able to identify precipitation, but also potentially the phase of the precipitation near the surface. Nevertheless, it should be reiterated that the amount of scattering by ice identified at these frequencies is not necessarily directly related to surface precipitation, and high amounts of water vapor in the atmospheric column above clouds or precipitation layer may negate any precipitation-related depression in the Tbs. Despite this, precipitation retrievals are still feasible from these channels particularly for intense precipitating systems, since surface precipitation rates and ice scattering signals are still strongly correlated in most convective systems.

3 ALGORITHM DESCRIPTION

The at-launch version of the TROPICS Precipitation Retrieval and Profiling Scheme (PRPS) utilized here is designed to provide a best-estimate of precipitation based upon *a priori* Tb-to-precipitation relationships derived from other satellite sensors. Post-launch versions will aim to utilize matchups between the TROPICS observations and the GPM DPR to inform and improve the *a priori* relationships. This fulfils in part the essence of GPM (and its predecessor, TRMM) in which the core observatory acts as a calibrator of precipitation retrievals for the international constellation of passive microwave instruments. In doing so the retrievals from the partner constellation sensors are able to provide greater temporal sampling and spatial coverage than is possible from the GPM satellite alone. However, the limitations of this approach are transferred through the retrieval scheme of the core satellite instrument to the resulting precipitation products. The availability of observations from the TROPICS pathfinder mission will allow the further development and testing of the retrieval scheme prior to the launch of the TROPICS constellation.

3.1. Algorithm Overview

The TROPICS precipitation retrieval scheme is the Precipitation Retieval and Profiling Scheme, described by Kidd et al. (2016, 2021). A fundamental design of the PRPS is the independence from any dynamic ancillary data sets (e.g. atmospheric or surface temperature from model reanalysis and other satellite products); i.e. the retrieval is based solely upon the satellite radiances linked to precipitation rates through a static *a priori* database and associated index file. This independence is advantageous when generating products across time scales from near real-time (inaccessibility to dynamic ancillary data, such as model data) to climatological scales (circumventing possible trends in such ancillary data).

The algorithm is designed to generate instantaneous estimates of precipitation at a constant resolution regardless of scan position (an approach adopted by Surussavadee and Staelin 2007), for all scan positions and scan lines. In addition to the precipitation estimate, an assessment of the error/uncertainty, a measure of the ‘fit’ of the observation to the database and a quality flag are provided.

3.2 Input Data

Three data inputs are required for the PRPS:

i) *a priori* database of (a minimum of) Tb radiances and associated precipitation rates;

ii) database index, and;

iii) Level 1 satellite observations.

The pre-launch TROPICS PRPS database comprises of an observation database based upon GPM DPR vs ATMS matches through utilizing the co-incident channels.

3.2.1 Observational database

The observational *a priori* databases used for the PRPS currently use coincident observations made by the GPM DPR (or TRMM PR) and the respective sensor. Since the observations from TROPICS is only available after launch an observational database has been generated using DPR-ATMS matchups, albeit using only the 4 co-incident channels, as shown in Table 2. The orbital tracks of the DPR and the ATMS are first analysed to find crossing locations that occur within 5 minutes of each other. These crossing points (as shown in Figure 3) are then used to find co-incident DPR and ATMS measurements (see Kidd et al. 2021). The DPR observations are averaged over a 3x3 window, the center of which is co-aligned with the ATMS footprint, thus providing a resolution of about 16.2 x 16.2 km (compared with 15.88 x 15.88 km best resolution of the ATMS at nadir).

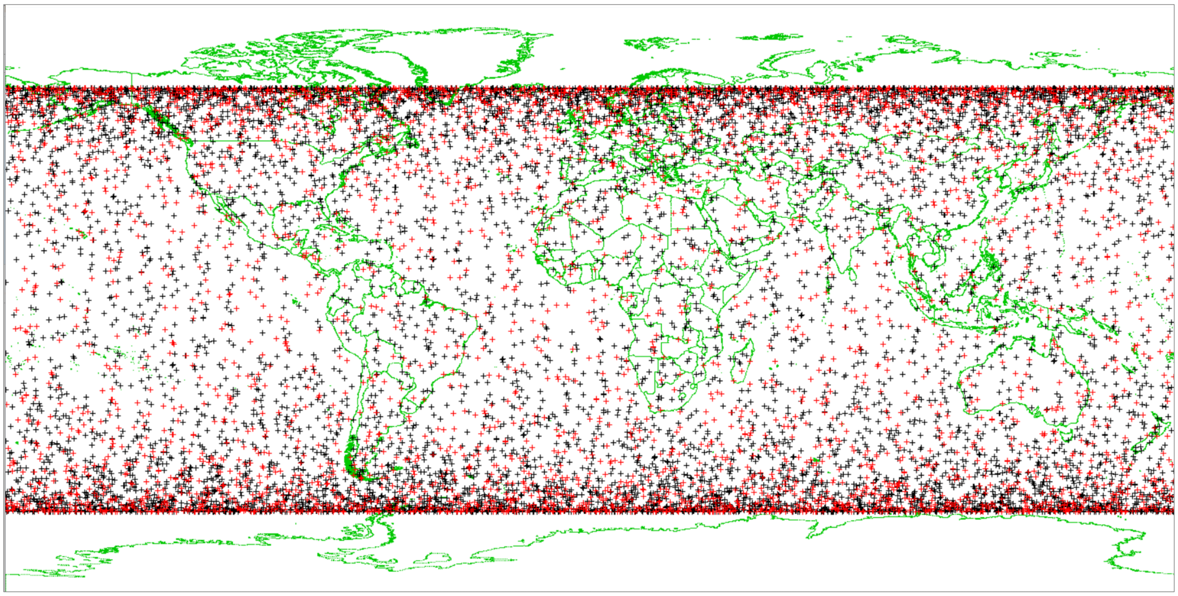

Figure 3: distribution of the DPR-ATMS orbital crossings used in the generation of the retrieval a priori database.

3.2.2 Database Index

To expedite the retrieval process in real time, the *a priori* databases are indexed based upon the two channels showing the greatest variance with each other. In this case channels 1 (TMS 91.655 GHz ≡ ATMS 89.5 GHz) and 9 (TMS 184.41 GHz ≡ ATMS 183.31± 1.0 GHz) are used, although the channels are not necessarily critical since they provide a first-guess. The index file describes the start and end point of the entries in the database array for a particular two-channel Tb combination, together with the number of entries for that combination. Accessing the relevant entries in the database is therefore merely looking up the starting entry (istart(Tb1, Tb2)) and ending entry (iend(Tb1,Tb2)). To ensure sufficient database entries are available for the retrieval search radius (within the (Tb1,Tb2) space) is set to obtain a minimum of 10,000 database entries. This approach provides a computationally efficient retrieval scheme .

3.2.3 Scan-position correction

Following on from the operational version of the PRPS-SAPHIR retrieval scheme (see Kidd et al. 2021) a similar correction methodology is applied to the TROPICS sensor. Since the scan angle is included in both the database and in the observations, only the database entries that have the same or similar scan angles to that of the observations are considered in the retrieval. This ensures that the characteristics of the resolution, incidence angle and atmospheric path are passed through from the database to the retrieval.

3.2.4 Level 1 data

Key input data from the L1 sensor data files include: i) date and time for each scan line (passed from the L1 files directly to the L2B output); ii) geolocation (lat/lon) data (values in group 1-3 and 4-5 are the same, the L2B data uses the 5^{th} group (see Table 3)); iii) L1B Tb data used in the generation of the retrieval; iv) the “Line-of-sight earth intersection longitude” and the L1B quality flag, used to determine if the data is within acceptable limits. Appendix A shows the list of the L1B data used in the retrieval, as defined in the netcdf data file structure.

Table 3: status of "calibration quality flag" used in the retrieval (see TROPICS Data User's Guide)

Bit	Meaning	Retrieval?
1	land/undefined	
2	Lunar/solar intrusion	Excluded
3	Active Maneuver Bit	Excluded
4	Cold Cal. Consistency	Excluded
5	Hot Cal. Consistency	Excluded
6	Ascending/Descending	
7	Day/Night	
8	Payload forward/aft	

3.3 Processing Outline

The processing stages are relatively straightforward and follow a sequential order of quality check, precipitation retrieval, error estimation and the generation of the 'fit' of the retrieval.

3.3.1 Quality check

The quality check array is set to 'missing' by default. If a scan/position exists, it is assumed that the retrieval is potentially good, and the quality flag is set to zero. A test is then undertaken to ascertain the validity of the input Tbs. This checks that the Tbs for each channel lie between 76 and 325 K; if one or more channel Tb lies outside this range the retrieval this is reflected in the quality flag, thus indicating that an issue has been detected. In addition, the L1B quality flags are used to check if the data was nominal (see below)

Table 4: L2B quality flags.

Flag value	Meaning
0	No issue – retrieval is good
-4	Tb flag – input data is out of bounds
-5	Land/sea mask is bad (unlikely)
-6	Lat/long of FOV is outside region (current set to 50S-50N
-7	Channel bad – one of the input channel Tbs is out of bounds
-8	Scan angle is bad (set when the nadir FOV exceeds -3 or 3 degrees)
-9	L1B data is flagged (for hot/cold calibration, solar or lunar intrusion).

3.3.2 Precipitation retrieval: database match

The database index file is initially interrogated to establish the start, end and the search radius associated with a particular 2-channel Tb combination. In this retrieval, the Tbs of channels 1 (91.655 GHz) and 9 (184.41 GHz) are used to find the starting and ending location of the relevant database entries from the database index, together with the search 'radius' (assuming the number of database enries for that Tb combination is less than 10,000). Each database entry within the specified range is compared against the observed Tbs, and the Euclidian distance calculated in Tb space. Each entry is ranked (1-6, based upon this distance) alongside the associated DPR rain rate (from the database). When the database search has finished, the 6 rain rates are then processed to generate the mean rain rate, error and 'fit' (see below). In addition, the most likely precipitation (the closest observation:database fit) is returned, along with its' Eculidan distance and the associated surface type (from the database).

3.3.3 Error estimate

In addition to the rain rate being generated from the mean of the 6 selected entries, the RMSE of these 6 rain rates is used to generate an 'error' estimate. Thus, if all 6 of the entries are similar a low error estimate is generated, while if the entries are disparate, a large error estimate is generated.

3.3.4 Fit of retrieval

A measure of the fit of the retrieval is also provided which is the RMSE of the (observed Tbs – database Tbs): this provides a measure of confidence in the representativeness of the retrieval.

3.4 Output data

The L2B output data therefore includes the date and time, geolocation, retrieved precipitation, measures of error and fit together with a quality flag. Appendix B shows the relevant netcdf dump of the pertinent data entries. Filenames are the same as for the L1B data except for L1B→L2B and BRTT→ISRR.

4 PRECIPITATION SCHEME TESTING AND EVALUATION

While ultimately the PRPS retrievals will be based upon a database comprised of TROPICS observations, an at-launch and immediate post-launch versions will not have, or ntot have sufficient observations to fully populate such a database.

As noted above, the current database for the PRPS-TMS is based upon 4-channels obtained from DPR-ATMS observations with about 18M entries. Nevertheless, at this stage, there are a reasonable number (2.8M) of DPR-TROPICS matches that allow use to evaluate whether the ATMS-based database is suitable as a substitute. This comparison can be done by investigating the Tb-surface rainfall relationships: in this case the mean Tb per rainrate category was calculate for both the DPR-ATMS observations and the DPR-TMS observations for each of the corresponding channels. The plots of these relationships are shown in Figure 4 below. While a perfect match between the ATMS and TMS-based would lie along the 1:1 line, the plots show that there is very good agreement between the two different sensor-rainrate relationships, and certainly high enough for a good degree of confidence in the retrieval scheme.

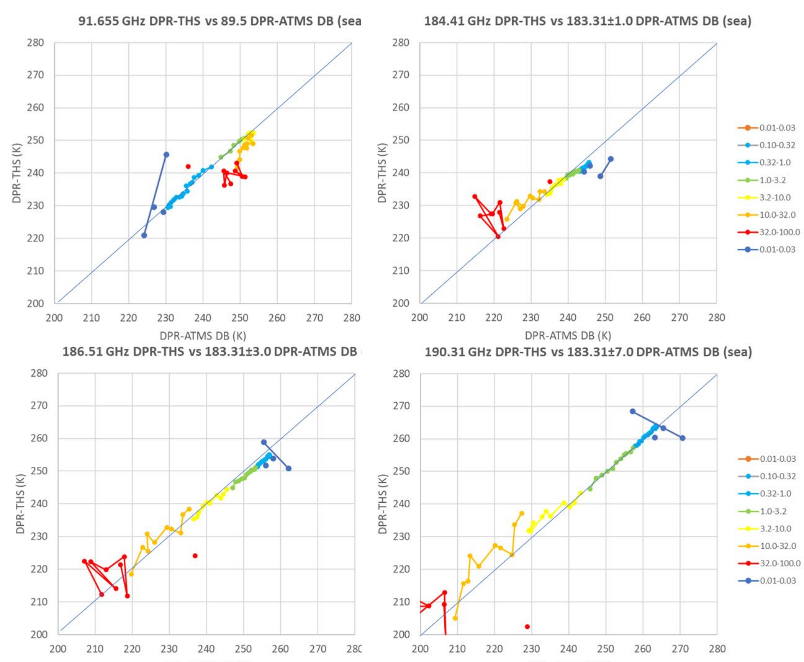

Figure 4: Plots of the Tb-rainrate relationships between the DPR-ATMS (horizontal axis) and the DPR-TMS (vertical axis), with the colours representing rainrates. (Only over sea areas have been chosen here due to the number of observations available from the TMS).

Further evaluation of the results have been carried out against the multi-satellite IMERG precipitation product (Figure 5). The specified requirements for the precipitation retrievals for the TROPICS mission is that the precipitation needs to be within 25% of the IMERG product at a spatial scale of 2.5 x 2.5 degrees and a temporal scale of 1 week (7-days). Two time periods were selected that met the necessary data quality requirements, these being 2021-08-08 through -14 and 2021-09-18 through -24. The comparison is shown in Figure xx below which shows the IMERG product (top), the TMS product (middle) and the different (bottom) for the first period (left) and the second period (right). The scatter plots in the center show the IMERG vs TMS mean precipitation intensity, with the thin solid blue lines defining the the 25% limits, and the thin dashed blue line showing the best-fit line through the data. For these cases the retrievals meet the required specifications.

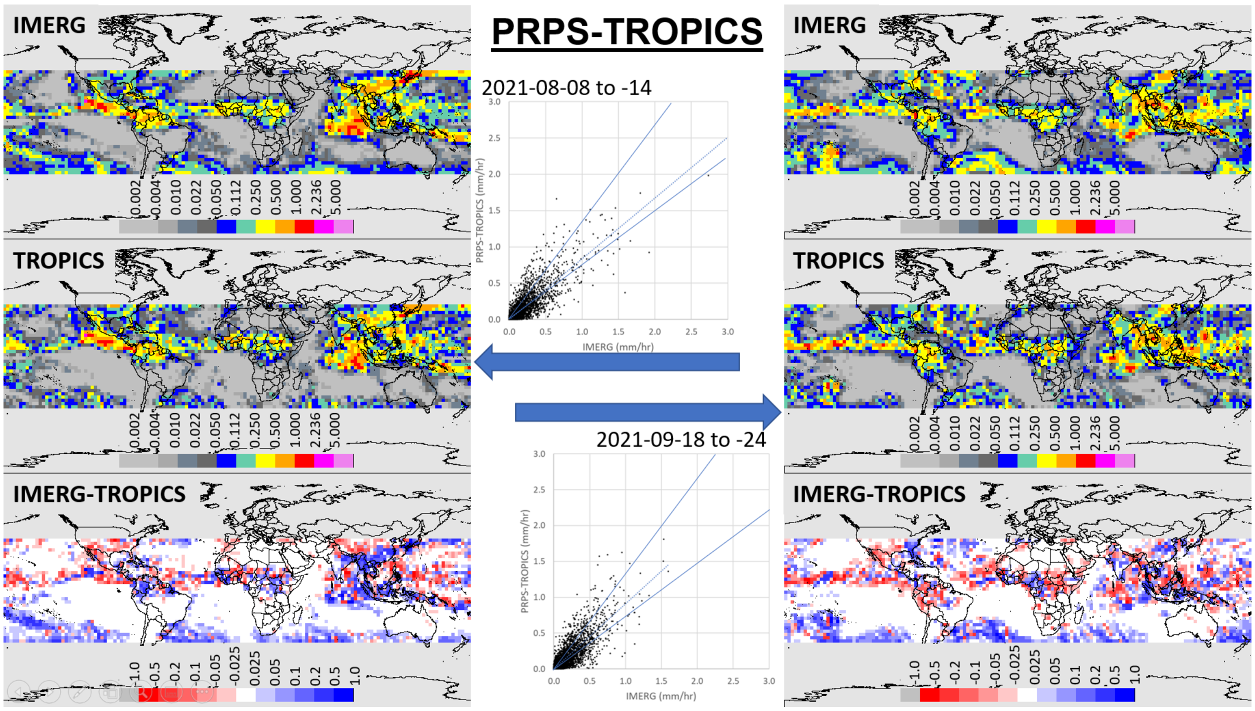

Figure 5: Comparison of the IMERG product (top), the TMS product (middle) and the different (bottom) for 2021-08-08 to -14 (left) and 2021-09-18 to -24 (right). The scatter plots in the center show the IMERG vs TMS mean precipitation intensity, with the thin solid blue lines defining the the 25% limits, and the thin dash blue line showing the best-fit line through the data.

A comparison of the same time periods with the retrievals made by the GPROF retrieval scheme using NOAA-19 data (with similar temporal sampling to TROPICS-pathfinder) show that the PRPS-TMS has comparable performance to the GPROF scheme (see Table 4 below).

Table 5. Statistical performance of the GPROF-NOAA19 retrievals vs IMERG and the PRPS-TMS retrievals vs IMERG for the two time periods.

IMERG vs GPROF-NOAA19

Period	ME	Ratio	RMSE	Correlation	Nobs
20210808-14	-0.0004	0.9968	0.0945	0.8921	4609.
20210918-24	-0.0049	0.9606	0.1010	0.8407	4609.

IMERG vs PRPS-TROPICS 0.4dev3, flagged data & DPR-ATMS database

Period	ME	Ratio	RMSE	Correlation	Nobs
20210808-14	-0.0073	0.9382	0.0993	0.8802	4609.
20210918-24	-0.0013	0.9891	0.1000	0.8535	4609.

In terms of instantaneous precipitation, four cases are shown below in Figure 6. These indicate that the PRPS-TMS provides a good indication of precipitation extent and intensity, certainly within the limitations of the instrumentation and channel selection. The scatterplots and statistical performance are similar to other instantaneous precipitation retrievals and show a reasonable performance for an initial post-launch version of a retrieval scheme.

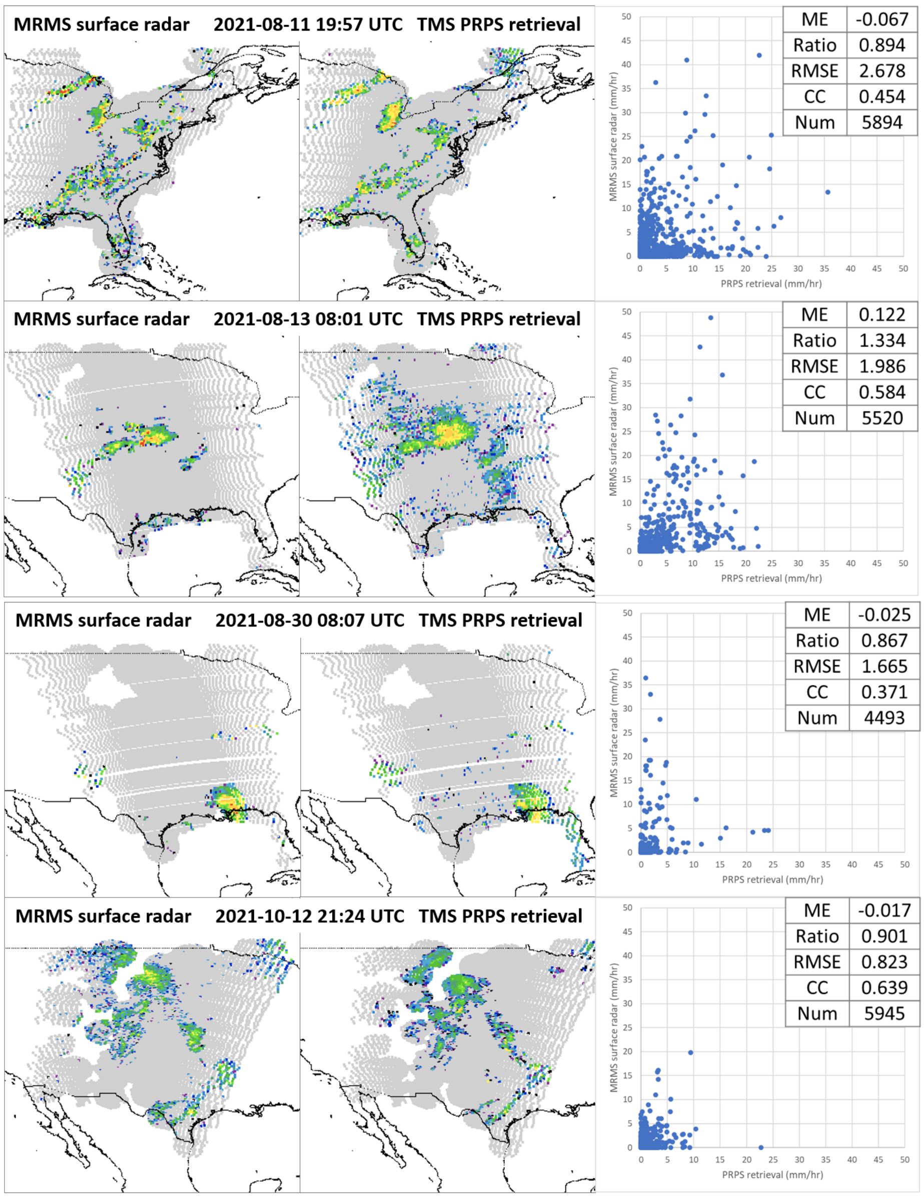

Figure 6: Comparisons of instantaneous PRPS-TMS retrievals vs MRMS surface radar over the US for four case studies.

4.1 Future development

At present the contribution of the O_2 channels to the precipitation retrieval are not included in the pre-launch retrieval scheme, although it is anticipated that these channels will be included once sufficient observations from TROPICS become available. An evaluation of a pre-launch retrieval scheme was performed using model-derived databases and HNR data which showed that the O_2 channels, particularly those away from the 118 GHz absorption band, could provide additional information on precipitation that could augment the currently used channels.

5. PRACTICAL CONSIDERATION

The current version of the PRPS scheme is considered to be the initial post-launch version, consequently there will be issues that arise with the accuracy of the final product. Users are encouraged to contact the providers to help refine and improve the products in later versions.

6. ASSUMPTIONS AND LIMITATIONS

The pre- and post-launch PRPS technique, like any other technique, is based upon a number of assumptions leading to limitations in the final product; these include:

- the currently database rain rates are based the DPR, and therefore the PRPS product is intrinsically linked to the accuracy of the DPR. As the PRPS is developed other satellite and surface products will be compared and incorporated with the aim of improving the overall accuracy of the retrievals;

- the resolution of the scan position is incorporated into the retrieval by considering only similar scan positions in the retrieval search, while each retrieval assume the same spatial resolution regardless of scan position;

- at present not all channels are exploited: pre-launch testing of the retrieval technique across all channels showed that the 118 GHz channel band had significantly higher variance than the 91.665, 183 and 204 GHz channels: at present it was decided to omit the 114-118 GHz channels from the retrievals, with the option of including them at a later stage.

- the current post-launch version does not include external dynamic data, relying solely upon the observed Tbs for the precipitation retrieval: external datasets may be considered in order to improve the accuracy of the product, particularly over certain regions.

7. REFERENCES

Blackwell, W.J., Braun, S., Bennartz, R., Velden, C., DeMaria, M., Atlas, R., Dunion, J., Marks, J., Rogers, R., Annane, B., Leslie, R.V. 2018: An overview of the TROPICS NASA Earth Venture Mission.Quart. J. Roy. Meteorol. Soc. 144, 16–26. https://doi.org/10.1002/qj.3290

Chern, J.-D., Tao, W.K., Lang, S. E., Li, X., and Matsui, T. 2020: Evaluating Precipitation Featuresand Rainfall Characteristics in a Multiscale Modeling Framework. J Adv. Modeling Earth Sys. 12, e2019MS002007. https://doi.org/10.1029/2019MS002007

Kidd, C. T. Matsui, J. Chern, K. Mohr, C. Kummerow, and D. Randall 2016: Global precipitation estimates from cross-track passive microwave observations using a physically-based retrieval scheme. Journal of Hydrometeorology, 17, 383–400. doi: http://dx.doi.org/10.1175/JHM-D-15-0051.1

Kidd, C., Matsui, T., and Ringerud, S. 2021a: Precipitation Retrievals from Passive Microwave Cross-Track Sensors: The Precipitation Retrieval and Profiling Scheme. Remote Sensing 13, 947. https://doi.org/10.3390/rs13050947

Matsui, T., Iguchi, T., Li, X., Han, M., Tao, W.-K., Petersen, W., L'Ecuyer, T., Meneghini, R., Olson, W., Kummerow, C.D., Hou, A.Y., Schwaller, M.R., Stocker, E.F. Kwiatkowski, J. 2013: GPM satellite simulator over ground validation sites, Bull. Amer. Meteor. Soc., 94, 1653–1660.

Tao, W.K., et al. 2009: A multiscale modeling system: Developments, applications, and critical Issues, Bull. Am. Meteorol. Soc., 90, 515–534, doi:10.1175/2008BAMS2542.1.

Tao, W.-K. and Chern, J. 2017: The impact of simulated mesoscale convective systems on global precipitation: A multiscale modeling study, Journal of Advances in Modeling Earth Systems, Vol 9, Issue 2, 790-809, https://doi.org/10.1002/2016MS000836

Matsui, T. T. Iguchi, X. Li, M. Han, W.-K. Tao, W. Petersen, T. L'Ecuyer, R. Meneghini, W. Olson, C. D. Kummerow, A. Y. Hou, M. R. Schwaller, E. F. Stocker, J. Kwiatkowski (2013), GPM satellite simulator over ground validation sites, Bull. Amer. Meteor. Soc., 94, 1653–1660. doi: http://dx.doi.org/10.1175/BAMS-D-12-00160.1

Surussavadee, C., and Staelin, D. H. 2007: Millimeter-Wave Precipitation Retrievals and Observed-versus-Simulated Radiance Distributions: Sensitivity to Assumptions, *Journal of the Atmospheric Sciences*, 64(11), 3808-3826. DOI: https://doi.org/10.1175/2006JAS2045.1

8 ACRONYMS

ATMS	Advanced Technology Microwave Sounder
DPR	Dual-frequency Precipitation Radar
FOV	Field of View
GPM	Global Precipitation Measurement (mission)
L1	Level 1 (data)
LEO	low Earth orbit
MHS	Microwave Humidity Sounder
PRPS	Precipitation Retrieval and Profiling Scheme
SAPHIR	Sondeur Atmosphérique du Profil d'Humidité Intertropicale par Radiométrie
Tb	brightness temperature
TMS	TROPICS Millimeter-wave Sounder
TRMM	Tropical Rainfall Measurement Mission
TROPICS	Time-Resolved Observations of Precipitation structure and storm Intensity with a Constellation of Smallsats (TROPICS)

APPENDIX A

L1B input data to retrieval scheme:

```
TROPICS01.BRTT.L1B.Orbit01352.V02-03.ST20210927-170942.ET20210927-184458.CT20220208-174340.nc

Dimensions: scans = 2859 (variable), spots = 81 (fixed), channels = 12 (fixed), bands = 5 (fixed)

        ushort Year(scans) ;
                Year:Long\ Name = "UTC year" ;
                Year:Description = "UTC year of the nadir spot." ;
                Year:Units = "years" ;
                Year:Valid\ Range = "2015-2030" ;
        ubyte Month(scans) ;
                Month:Long\ Name = "UTC month" ;
                Month:Description = "UTC month of year for the nadir spot." ;
                Month:Units = "months" ;
                Month:Valid\ Range = "1-12" ;
        ubyte Day(scans) ;
                Day:Long\ Name = "UTC day" ;
                Day:Description = "UTC day of month for the nadir spot." ;
                Day:Units = "days" ;
                Day:Valid\ Range = "1-31" ;
        ubyte Hour(scans) ;
                Hour:Long\ Name = "UTC hour" ;
                Hour:Description = "UTC hour of day for the nadir spot." ;
                Hour:Units = "hours" ;
                Hour:Valid\ Range = "0-23" ;
        ubyte Minute(scans) ;
                Minute:Long\ Name = "UTC minute" ;
                Minute:Description = "UTC minute of hour for the nadir spot." ;
                Minute:Units = "minutes" ;
                Minute:Valid\ Range = "0-59" ;
        ubyte Second(scans) ;
                Second:Long\ Name = "UTC second" ;
                Second:Description = "UTC second of minute for the nadir spot." ;
                Second:Units = "seconds" ;
                Second:Valid\ Range = "0-59" ;
        ushort Millisecond(scans) ;
                Millisecond:Long\ Name = "UTC millisecond" ;
                Millisecond:Description = "UTC millisecond of second for the nadir spot." ;
                Millisecond:Units = "milliseconds" ;
                Millisecond:Valid\ Range = "0-999" ;
        float tempBrightE_K(channels, scans, spots) ;
                tempBrightE_K:_FillValue = -999.f ;
                tempBrightE_K:Long\ Name = "Earth radiometric brightness temperature" ;
                tempBrightE_K:Description = "Planck blackbody equivalent brightness temperatures"
;
                tempBrightE_K:Units = "kelvins" ;
                tempBrightE_K:Valid\ Range = "0-350" ;
        double timeE(scans, spots) ;
                timeE:Long\ Name = "Time of Earth radiometric measurements" ;
                timeE:Description = "TROPICS Epoch Time (TET) timestamp of the Earth radiometric
measurements." ;
                timeE:Units = "TET is the number of atomic seconds elapsed since January 1, 2000
00:00:00.000 TAI" ;
                timeE:Valid\ Range = "6.7e+09" ;
        float losLat_deg(bands, scans, spots) ;
                losLat_deg:_FillValue = -999.f ;
                losLat_deg:Long\ Name = "Line-of-sight earth intersection latitude" ;
```

```
                losLat_deg:Description = "Geodetic latitude of the line-of-sight intersection
point with the Earth. Negative values are South. These correspond to the middle of each spot\'s
integration period. WGS84" ;
                losLat_deg:Units = "degrees" ;
                losLat_deg:Valid\ Range = "-90 to 90" ;
        float losLon_deg(bands, scans, spots) ;
                losLon_deg:_FillValue = -999.f ;
                losLon_deg:Long\ Name = "Line-of-sight earth intersection longitude" ;
                losLon_deg:Description = "Geodetic longitude of the line-of-sight intersection
point with the Earth. Negative values are West. These correspond to the middle of each spot\'s
integration period. WGS84" ;
                losLon_deg:Units = "degrees" ;
                losLon_deg:Valid\ Range = "-180 to 180" ;
        float losScan_deg(bands, scans, spots) ;
                losScan_deg:_FillValue = -999.f ;
                losScan_deg:Long\ Name = "Line-of-sight scan angle" ;
                losScan_deg:Description = "The scan angle between the satellite local nadir and
the Line-Of-Sight (LOS) vector from radiometer aperture." ;
                losScan_deg:Units = "degrees" ;
                losScan_deg:Valid\ Range = "0-180" ;
        ubyte calQualityFlag(channels, scans, spots) ;
                calQualityFlag:Long\ Name = "Calibration Quality Flag" ;
                calQualityFlag:Description = "See TROPICS Data User\'s Guide. Bit 1:
land/undefined Bit 2: Lunar/solar intrusion Bit 3: Active Maneuver Bit 4: Cold Cal. Consistency
Bit 5: Hot Cal. Consistency Bit 6: Ascending/Descending Bit 7: Day/Night Bit 8: Payload
forward/aft" ;
                calQualityFlag:Units = "unitless" ;
                calQualityFlag:Valid\ Range = "0 to 128" ;
        ubyte LandFlag(scans, spots) ;
                LandFlag:Long\ Name = "Land Flag" ;
                LandFlag:Description = "0 is ocean, 1 is land or coastline, and 2 is bad or
undefined" ;
                LandFlag:Units = "unitless" ;
                LandFlag:Valid\ Range = "0 to 3" ;
```

APPENDIX B

PRPS L2B output:

```
TROPICS01.ISRR.L2B.Orbit01352.V01-01.ST20210927-170942.ET20210927-184458.CT20220215-174308.nc

dimensions: scans = 2859 (variable), spots = 81 (fixed)

        double timeE(scans, spots) ;
                timeE:Long\ Name = "Earth radiometric measurement time" ;
                timeE:Description = "Elapsed GMT timestamp of the Earth radiometric
measurements." ;
                timeE:units = "Seconds since 1/1/1970 00:00.000.  Leap seconds are already
subtracted." ;
                timeE:Valid\ Range = "1.5778e+09-1.8935e+09" ;
        ushort Year(scans) ;
                Year:long\ name = "UTC year" ;
                Year:description = "UTC year of the nadir spot." ;
                Year:units = "years" ;
                Year:valid\ range = "2015-2030" ;
        ubyte Month(scans) ;
                Month:long\ name = "UTC month" ;
                Month:description = "UTC month of year for the nadir spot." ;
                Month:units = "months" ;
                Month:valid\ range = "1-12" ;
        ubyte Day(scans) ;
                Day:long\ name = "UTC day" ;
                Day:description = "UTC day of month for the nadir spot." ;
                Day:units = "days" ;
                Day:valid\ range = "1-31" ;
        ubyte Hour(scans) ;
                Hour:long\ name = "UTC hour" ;
                Hour:description = "UTC hour of day for the nadir spot." ;
                Hour:units = "hours" ;
                Hour:valid\ range = "0-23" ;
        ubyte Minute(scans) ;
                Minute:long\ name = "UTC minute" ;
                Minute:description = "UTC minute of hour for the nadir spot." ;
                Minute:units = "minutes" ;
                Minute:valid\ range = "0-59" ;
        ubyte Second(scans) ;
                Second:long\ name = "UTC second" ;
                Second:description = "UTC second of minute for the nadir spot." ;
                Second:units = "seconds" ;
                Second:valid\ range = "0-59" ;
        ushort Millisecond(scans) ;
                Millisecond:long\ name = "UTC millisecond" ;
                Millisecond:description = "UTC millisecond of second for the nadir spot." ;
                Millisecond:units = "milliseconds" ;
                Millisecond:valid\ range = "0-999" ;
        float losLat(scans, spots) ;
                losLat:description = " latitude A/B-scan (-90:90)" ;
                losLat:units = "[deg]" ;
         float losLon(scans, spots) ;
                losLon:description = " longitude A/B-scan (-180:180)" ;
                losLon:units = "[deg]" ;
         float rain_rate(scans, spots) ;
                rain_rate:description = "PRPS derived rain rates" ;
                rain_rate:units = "[mm/hr]" ;
                rain_rate:Fillvalue = "-999.f" ;
        float rain_rmse(scans, spots) ;
                rain_rmse:description = "RMSE retrieved precipitation" ;
```

```
        rain_rmse:units = "[-]" ;
        rain_rmse:Fillvalue = "-999.f" ;
float tb_fit(scans, spots) ;
        tb_fit:description = " fit of Tbs of the retrieved value to database Tbs" ;
        tb_fit:units = "[K]" ;
        tb_fit:Fillvalue = "-999.f" ;
float MLP_rate(scans, spots) ;
        MLP_rate:description = " Most Likely Precipitation" ;
        MLP_rate:units = "[mm/hr]" ;
        MLP_rate:Fillvalue = "-999.f" ;
float surface_type(scans, spots) ;
        surface_type:description = " retrieved surface type" ;
        surface_type:units = "none" ;
        surface_type:Fillvalue = "-999.f" ;
float Tb_fitMLP(scans, spots) ;
        Tb_fitMLP:description = " fit of Tbs of the retrieved MLP to database Tbs" ;
        Tb_fitMLP:units = "[K]" ;
        Tb_fitMLP:Fillvalue = "-999.f" ;
byte prps_flag(scans, spots) ;
        prps_flag:description = " quality flag: zero=OK" ;
        prps_flag:units = "[-]" ;
        prps_flag:Fillvalue = "-9" ;
```